Progress In Electromagnetics Research, PIER 50, 41–60, 2005

APPARENT RADAR CROSS SECTION OF A LARGE TARGET ILLUMINATED BY A SURFACE WAVE ABOVE THE SEA

V. Fabbro

ONERA-DEMR
2 avenue Edouard Belin, 31055 Toulouse Cedex 4, France

P. F. Combes

UPS-AD2M-IGEEP
118 route de Narbonne, 31062 Toulouse Cedex 4, France

N. Guillet †

ONERA-DEMR
2 avenue Edouard Belin, 31055 Toulouse Cedex 4, France

Abstract—Classical assesssment of the received power by a radar leads to a decorrelation of many relevant phenomena (i.e. propagation, backscattering), which may introduce modelling errors notably in the presence of large target with respect to the wavelength. To overcome this limitation, a new hybrid approach is proposed. It combines a method of propagation calculation (the parabolic wave equation) with a method of scattering calculation (the EFIE solved by a method of moment approach) and an application of the reciprocity principle (the power coupling factor). Each method constituting the hybrid approach is described; the example of a large cargo is chosen and its apparent RCS is evaluated above the sea at low frequency. The results are discussed, studying the influence of the different parts of the boat on the apparent RCS.

† Also with UPS-AD2M-IGEEP, 118 route de Narbonne, 31062 Toulouse Cedex 4, France

1. INTRODUCTION

Propagation phenomena consideration for coverage predictions in the radar or telecommunication domain proves to be increasingly important. According to frequency and environment properties, different phenomena can be observed such as surface wave above the sea (at a low frequency of a few Megahertz) or trapping effect in ducting conditions (at high frequency of a few GigaHertz) when a trapping layer exists, involving a negative M-unit gradient in the low altitude atmosphere. These conditions strongly affect the radar and communication performances as evidenced by increased or decreased detection and communication ranges.

The genesis of the current generation of Over The Horizon Radars systems (OTH), and in particular the HF Surface Wave Radars (HFSWR) started in the 1960s [1]. The navy's system's have been upgraded [2, 3], and powerful algorithms and methods of simulation were used for improving the performance of these systems. Nevertheless, fundamental problems are remaining as detection and tracking in clutter dominated environment [4, 5]. Then the topic of improving the radar returns from ship at low frequency continues to be of current interest in both defense and civil sector. Over several years, efficient propagation prediction tools for operational applications have been developed and validated [6–8], as well as robust tools for the scattering computation [9, 10]. The assessment of the power received by a radar antenna, is then classically achieved by the following radar equation:

$$P_r = \frac{P_t G^2 \lambda^2}{(4\pi)^3 R^4} f_a^4 F^4 \sigma_{fs} \tag{1}$$

P_t is the transmitted power, G the antenna gain in transmission and reception mode, λ the wavelength, R the antenna-target range, f_a the antenna pattern, F the propagation factor (traducing the propagation effects by reference to the free space conditions) and σ_{fs} the Radar Cross Section (RCS) in free space conditions.

In this equation the main approximation *is the decorrelation between the different physical phenomena* such as the propagation and the backscattering. The RCS computation is in general carried out for an incident plane wave and this constitutes another approximation because in real conditions the incident wave is not a plane wave. In most classical coverage prediction assessment, the propagation effects are expressed by the propagation factor F and the target is considered as a point where F is computed. This approximation is questionable for a target larger than the wavelength. Indeed, if this approach is a good approximation when the target has low dimensions with respect to the wavelength, it can lead to significant errors on the modelled backscattered power when large target, such as a boat or a plane are considered. Without these approximations this problem has been considered in two dimensions [11] using integral equation approach (the Generalised Forward Backward method) to study for example the rough sea influence on the RCS of a two dimensional ship. But to consider a real three-dimensional target and all the propagation effects (including refraction) for large domains and large targets is a hard problem, for which most of the methods apply an inconsistent approach uncoupling propagation and backscattering.

Another idea would be to use a decomposition of the large target by a series of scatterers. In this case, the propagation factor can be computed at each point and the total response of the target is the sum of each contribution. But in this approach there is another approximation: the relative phases of the incident field on each point are often ignored. Moreover, the scatterers decomposition is function of the frequency and the orientation of the target, so the decomposition must be computed for each configuration considered.

In this paper a coherent approach is proposed to avoid all these approximations, taking into account simultaneously the antenna, the propagation and backscattering effects. This global approach is based on an hybridization between: the parabolic wave equation method (PWE) for the propagation and a method of moment solving the EFIE (Electrical Field Integral Equation) for the target backscattering. Fig. 1 gives a representation of this hybrid scheme. Using this

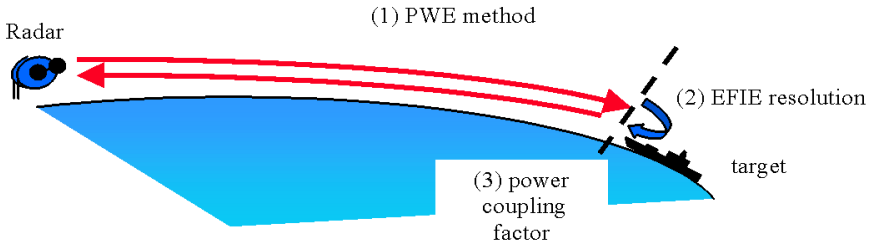

Figure 1. Scheme showing the three methods constituting the hybrid method for the computation of the apparent RCS of a target.

hybridization, the apparent Radar Cross Section σ_a is evaluated and can be substituted to the analytical and inconsistent expression $f_a^4 F^4 \sigma_{fs}$ (see equation (1)) of the classical approach. In this coherent approach, the radar equation becomes:

$$P_r = \frac{P_t G^2 \lambda^2}{(4\pi)^3 R^4} \sigma_a \tag{2}$$

In such a way the PWE method computes the electromagnetic field incident on the target, and the EFIE method works out the currents on the target and their radiation pattern. It is worth noticing that the computation of the return path may be avoided using the reciprocity principle through the power coupling factor as in [12, 13]. The decomposition of the hybrid method is then (see Fig. 1): (1) the PWE method, (2) EFIE method and (3) the power coupling factor method.

In this paper, the hybrid method is applied for Surface Wave Radar detection used in an integrated Marine surveillance system. This method allows us to take into account in a coherent approach all the propagation phenomena at low frequency (surface wave, recovery effect) and the target, for full sea or coastal configurations. To prove the advantage of the proposed approach, some examples on a large target are presented. This target is a cargo, illuminated by a surface wave above the sea surface at low frequency (i.e., a few Megahertz). To explain the target response to its illumination, the cabin and the bottom contributions of the boat are compared. The results are

presented and confronted to the classical approach described by (1) with a significant improvement since the actual variations of the target illumination law by the incident surface wave are taken into account.

2. PROPAGATION MODELLING

2.1. Parabolic Equation Method and Leontovitch Boundary Condition

Nowadays the PWE method is recognized as the more efficient 2D method to model the propagation in a coastal environment. Its main advantage is its computational time with a split-step Fourier resolution and its large frequency range of validity from a few megahertz, to several tens of gigahertz. The PWE resolution approach chosen is the Discrete Mixed Fourier Transform (DMFT) developed by Dockery, Kuttler and Donohue [14–16]. The basic equation is the wide angle PWE of the form:

$$\frac{\partial \Phi}{\partial x} = j\sqrt{k_o^2 + \frac{\partial^2}{\partial z^2}}\Phi + jk_o m(x,z)\Phi \tag{3}$$

Where x is the horizontal range, z the altitude, k_o the free-space wave number, $m(x,z)$ the modified refractive index and $\Phi(x,z)$ the transverse electric or magnetic field for horizontal or vertical polarisation, respectively. The Split-Step Fourier method (SSF) allows a recursive resolution following the formulation given below:

$$\Phi(x+\delta x, z) = e^{j\frac{k_o}{2}m(x,z)\delta x} TF^{-1}\left\{ e^{j\sqrt{k_o^2-p^2}\delta x} TF\left[e^{j\frac{k_o}{2}m(x,z)\delta x}\Phi(x,z)\right]\right\} \tag{4}$$

TF is the a Fourier type Transform, p the dual of z in the spectral domain and δx the horizontal step length.

To model the propagation above perfectly conducting surfaces, according to the wave polarisation, the boundary conditions of Dirichlet (horizontal polarisation) or Neumann (vertical polarisation) have to be enforced. However, for many problems considering the ground as perfectly conducting is not a good approximation. A solution is to introduce the Leontovitch boundary condition [14] using a realistic surface impedance.

The Leontovitch boundary condition [17] can be written dependent on the polarisation as follows:

$$\left.\frac{\partial \Phi}{\partial z}\right|_{z=0} + \alpha_{H,V}\Phi|_{z=0} = 0 \tag{5}$$

The term α can be directly obtained at low grazing angles and is defined by:

$$\alpha_{H,V} = jk_o\delta_{H,V} \text{ where } \delta_{H,V} \text{ is} \tag{6}$$

$$\begin{cases} \delta_V = \dfrac{\sqrt{\eta - 1}}{\eta} \text{ (Vertical Polarisation)} \\ \delta_H = \sqrt{\eta - 1} \text{ (Horizontal Polarisation)} \\ \text{With } \eta = \varepsilon_r + j60\sigma\lambda \end{cases} \tag{7}$$

ε_r and σ are the ground permittivity and conductivity. With these expressions one can introduce the roughness of the surface in the propagation computation through the parameter.

In the case of propagation above the sea at a few Megahertz, the Rayleigh roughness parameter and the surface slopes are much smaller than unity. So the small perturbation method can be applied to compute the surface impedance of the rough surface. The formula of the modified impedance surface has been derived by Barrick [18, 19] applying the second order small perturbation method with the Leontovitch approximation.

$$\bar{\Delta} = \Delta + A \tag{8}$$

Where A represents a double integral in the spectral domain given by:

$$A = \frac{1}{4}\int_{-\infty}^{+\infty}\int_{-\infty}^{+\infty} F(p,q)W(p,q)dpdq \tag{9}$$

With

$$F(p,q) = \frac{p^2 + b'\Delta(p^2 + q^2 - k_0 p)}{b' + \Delta(b'^2 + 1)} + \Delta\left(\frac{p^2 - q^2}{2} + k_0 p\right) \tag{10}$$

And

$$b' = \frac{1}{k_0}\sqrt{k_0^2 - (p + k_0)^2 - q^2} \tag{11}$$

p and q are the dual variables of x and y in the Fourier space, $W(p,q)$ represents the gravity spectrum. The sea is considered as created by the wind and described by the Phillips spectrum [20]:

$$W(p,q) = \frac{2.10^{-2}}{\pi(p^2 + q^2)^2} \tag{12}$$

Let us notice that the PWE resolution method by the DMFT allows to take into account all the ground effects through the Leontovitch boundary condition, including the surface wave at low frequency and the recovery effect which can be observed above a surface when its dielectric properties change from lossy to conductor (as from land to sea surface).

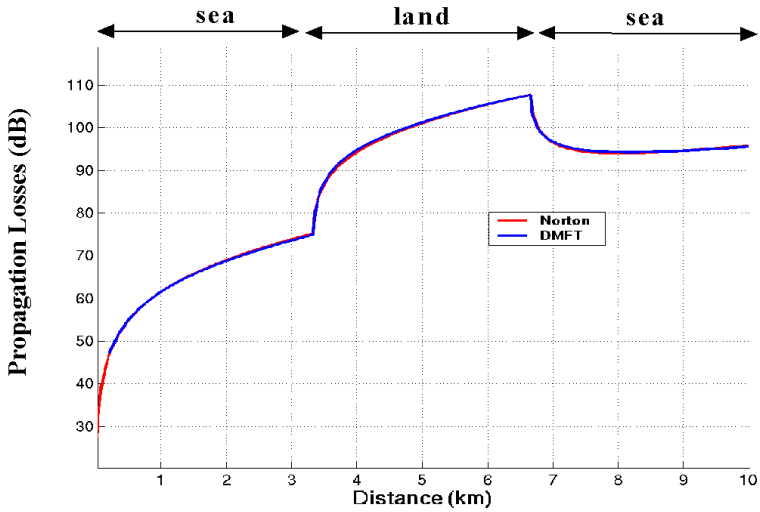

Figure 2. Propagation losses showing the recovery effect on an inhomogeneous propagation path: sea – land – sea.

2.2. Example of Recovery Effect

For the low frequencies of a few Megahertz considered in this study, one of the most interesting propagation phenomenon discovered is the surface wave above the sea and the recovery effect observed in coastal environment. The surface wave can be strong and dominant when the transmitter is near the sea surface and a recovery effect (also called Millington effect [21, 22]) can appear when a transition between land and sea surface is met. It is characterised on the propagation path by an increase of the propagation losses above the land path and a decrease of the propagation losses above the sea. To illustrate this phenomenology a simple example is presented above. The frequency considered is 50 Mhz and the transmitter is at the sea surface. The path losses are computed using the DMFT algorithm to a maximum range of 10 kilometres. Fig. 2 is a representation of these propagation losses versus the distance, the observation being chosen at the altitude of zero meters, i.e. at the boundary of the computational domain. From 0 to 3.3 kilometres and from 6.6 to 10 kilometres, the propagation losses are computed above sea water (characterised by a relative permittivity and a conductivity respectively of $\varepsilon_r = 80$ and $\sigma = 4\,\mathrm{S/m}$); from 3.3 to 6.6 kilometres the propagation losses are computed above a wet land (characterised by $\varepsilon_r = 4$ and $\sigma = 10^{-2} S/m$). On the three first

kilometres, above the sea, the propagation is dominated by the surface wave and this wave disappears above the land and reappears above the sea for the last part of the path. The propagation losses clearly show this behaviour, strongly growing above the land from 3.3 kilometres, and decreasing from 6.6 kilometres above the last part of sea surface. On Fig. 2, the DMFT results have been compared to the asymptotic approach developed by Norton [23, 24] for a transmitter that is a small dipole. The results are in perfect agreement and the recovery effect is very well modelled by the two approaches.

3. RCS CALCULATION

In most of the modelisations of the target RCS in its environment, approximations on the shape and construction of the target (aircraft or boats [2]) are introduced. The main interest of the proposed approach is to compute the apparent RCS considering the actual incident wave with its phase and amplitude variations and not a plane wave as most of the authors usually do. The two steps of this determination are: first the computation of the backscattering on an interface situated close to the target and secondly the propagation backward to the radar antenna using a power coupling factor.

3.1. Target Backscattering Computation

One solution would be to decompose the incident wave in a plane wave spectrum using a Fourier Transform and to apply a classical method as physical optics to compute the scattering of each incident plane wave [13, 25]. Then the total scattered field would be computed from the sum of elementary scattered fields corresponding to each incident plane wave. This method can give accurate results but may lead to prohibitive computation time or memory size for large targets. We prefer to use a resolution of the Electric Field Integral Equation (EFIE) [26, 27] which allows to compute the scattered field by the target after the determination of the induced currents $\vec{J}$ on this target by a non-uniform incident wave. In the case of a metallic object, we can use the boundary condition on the surface:

$$\vec{n} \times \vec{E} = 0 \tag{13}$$

Where $\vec{n}$ is perpendicular to the surface and $\vec{E}$ is the total field. This condition explains that the tangential total field is zero on the surface. With this hypothesis and applying the equivalence principle, an integral equation is obtained [28] giving the exact value of the

induced currents by the incident wave as:

$$\vec{n}\times\vec{E_{inc}} = j\frac{\omega\mu_0}{k_0^2}\vec{n}\times\vec{grad}div\int_S \vec{J}.G(R)ds + j\omega\mu_0\vec{n}\times\int_S \vec{J}.G(R)ds \quad (14)$$

Where G the Green function of free space at the distance R, and $\vec{E}_{inc}$ the incident field.

To determine the induced current, a basis of functions is written to represent it. The above equation is projected on this basis. In such a way, a matrix system is obtained that must be inverted to compute the currents on the object surface. Once the currents are known, their radiation is computed and propagated to the observation points. This calculation is made by the ONERA tool: ELSEM3D [9, 26]. All the theory of the EFIE resolution used is well known and is not reported here [27]. The scattering object is described by a mesh composed of triangular or quadrangular patches for the surfaces and of segments for the edges (an example is given Fig. 3). The size of each element must be lower than the incident wavelength divided by six to accurately represent the variations of the electromagnetic field. The scattered field is propagated in free space from the target to the observation points; moreover the image principle, considering the ship and its image, is applied to take into account the hypothetical case of a smooth and conducting sea. This restrictive hypothesis is nevertheless acceptable in so far as the scattered field is computed at a target-observation range much lower than the far zone of the ship which may be very large. Now

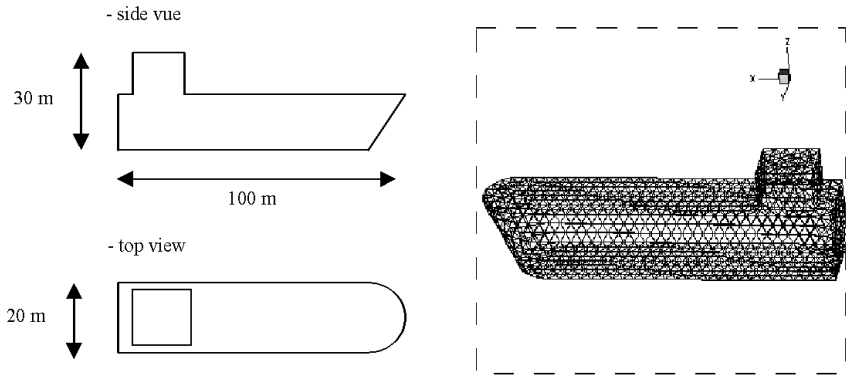

Figure 3. Target sizes and mesh representation for the EFIE scattering computation.

the propagation effects on the return path can be taken into account through a powerful application of the reciprocity principle as described below.

3.2. Application of the Reciprocity Principle

Applying the reciprocity principle, the return path calculation can be avoided. This approach consists in computing — along a two dimensional interface near the target — a scalar product called coupling factor [12], between the incident field E_1 from the antenna (obtained by the PWE method) and the target backscattered field E_2 (obtained by the EFIE method). This coupling factor allows to calculate the backscattered power to the radar antenna and then to deduce the apparent RCS of the target. A schematic illustration of the connection on the coupling interface between the components E_1 and E_2 is shown in Fig. 4.

If one refers to the theory of antennas, transmitting and receiving modes can be correlated by the reciprocity principle applied on an interface. Thus, the power P delivered to the antenna load can be derived from the power density p_2 backscattered on the interface by:

$$P = S_a \gamma_c \; p_2 \tag{15}$$

Where, S_a is the effective area of the radar antenna and γ_c is the power coupling factor:

$$\gamma_c = \frac{|\langle E_2, E_1 \rangle|}{\|E_1\|^2 \|E_2\|^2} \tag{16}$$

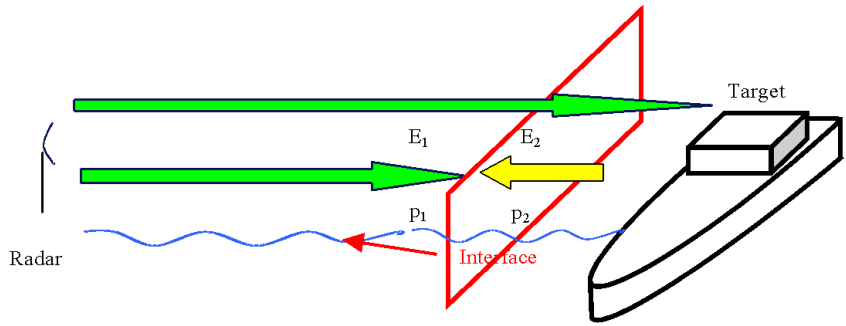

Figure 4. Schematic illustration of the methodology for the power coupling factor computation, along a vertical interface.

E_1 and E_2 are the transverse electric fields respectively radiated on the interface by the antenna and by the target (see Fig. 4). These fields can be expressed from the power densities p_1 and p_2 (W/m^2) by:

$$|E_1\|^2 = 2Z_0 p_1 \text{ And } \|E_2\|^2 = 2Z_0 p_2 \tag{17}$$

Z_0 is the wave impedance approximated to the free space wave impedance.

Then, from equations (15), (16), (17) the power P delivered to the antenna load can be expressed as a function of: the radiated power density p_1 by the antenna in the transmitting mode, the effective area of the antenna, and the scalar product on the interface between the incident and backscattered field according to:

$$P = \frac{|\langle E_2, E_1\rangle|^2}{p_1(2Z_0)^2} S_a \tag{18}$$

In the second term of this equality, the only function depending on the environment is the scalar product $|\langle E_2, E_1\rangle|$ (because Z_0 is everywhere assumed as very close to the free space wave impedance). If the same configuration is considered with two different propagation conditions, such as free space and a realistic environment, the ratio between the power transmitted to the load can be derived from the scalar products ratio:

$$\frac{P_{real}}{P_{fs}} = \frac{|\langle E_{2real}, E_{1real}\rangle|^2}{|\langle E_{2fs}, E_{1fs}\rangle|^2} \tag{19}$$

Where *real* is for realistic environment and fs is for free space environment. The antenna characteristics being identical in the two environments, one can see from (2) that the power transmitted ratio is equal to the apparent RCS ratio :

$$\frac{\sigma_{a\,real}}{\sigma_{a\,fs}} = \frac{|\langle E_{2real}, E_{1real}\rangle|^2}{|\langle E_{2fs}, E_{1fs}\rangle|^2} \tag{20}$$

Assuming that the apparent RCS in free space is known, the apparent Radar Cross Section in the realistic environment is immediately derived using equation (20). The only hypothesis considered in the Power coupling factor theory is that the forward and backward path environments are identical. This is justified considering the very high speed of the electromagnetic wave with respect to the environment variation speed. In an alternative process, the return path computation could be performed using the PWE method between the interface and the radar antenna. One can remind that we use a two dimensional resolution of the PWE; so to initialize on the interface the PWE

resolution, an hypothesis of azimutal invariability must be considered between the target and the interface (see Fig. 4). To be sure that all the transverse effects can be neglected, the interface must be chosen in the far zone of the target. This is a problem because the far zone of the ship is very large, and moreover, the backscattering computation is made by the EFIE method which considers a free space propagation between the target and the interface (and consequently does not take into account the surface wave above has the sea surface). *So the method we propose, with the coupling factor, has to be preferred because in this method the interface may be near the target and the range where one considers free space conditions for the propagation is short.*

4. HYBRID METHOD APPLICATION ON A CARGO

The goal is to demonstrate the limits of the classical approach (obtained by equation (1)) on complex target even at low frequency by comparison to the proposed coherent hybrid method (explained by equation (2)). The target chosen to realise the study is a cargo whose shape is taken more simplified than a real one to facilitate all the physical interpretations of the results; but the same hybrid method can be applied to a more sophisticated target without any problem. Fig. 3 shows a graphic representation of the target mesh and sizes.

The apparent RCS is studied in two bistatic configurations where the transmitter and the cargo are motionless and the receiver moves in azimuth around the cargo. Both configuration correspond to two different orientations of the ship (as shown in Fig. 5 and Fig. 6) .

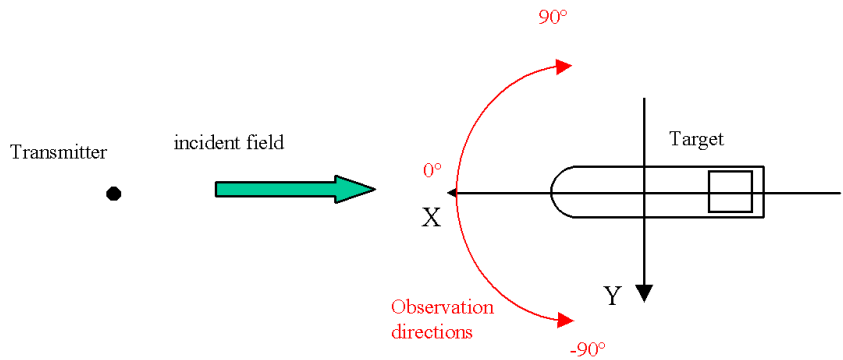

Figure 5. First bistatic configuration: the incident field illuminates the prow and the receiver moves in azimuth around the cargo.

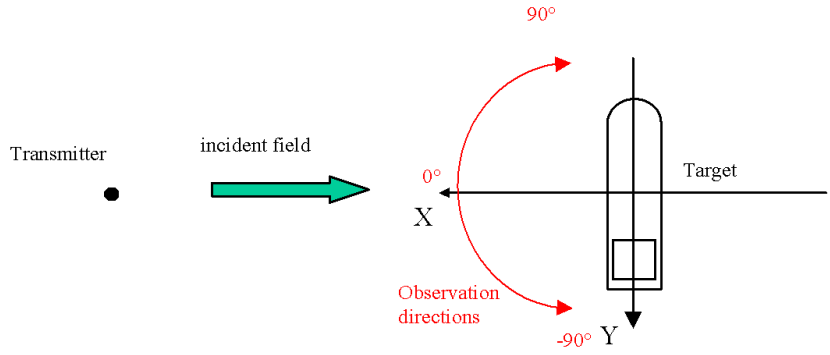

Figure 6. Second bistatic configuration: the incident field illuminates the cargo side and the receiver moves in azimuth around.

The study is lead at a frequency of 50 Megahertz, when the cargo is illuminated by a surface wave above the sea.

Fig. 7 shows two graphs describing the incident wave on the target. This wave is radiated by a vertical dipole above the sea at a height of 20 meters, allowing a vertical polarisation of the incident wave. A sea state corresponding to a wind of 15 m/s is considered in the propagation modelling through the Barrick impedance (see equation (8)). On the left Fig. 7, the propagation losses in dB are represented against the height and the distance. The surface wave above the sea

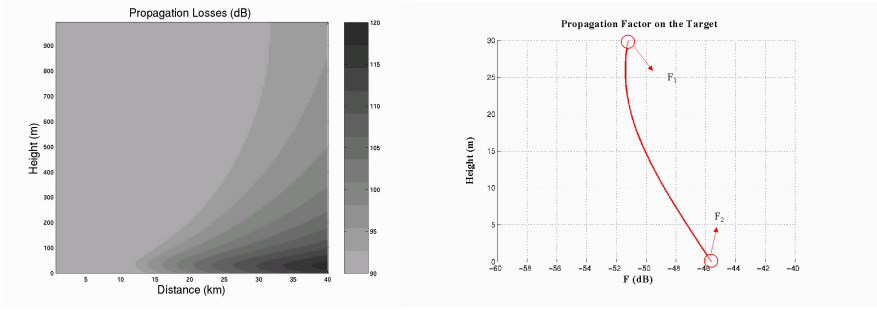

Figure 7. Graphs describing the incident wave on the cargo: on the left, propagation losses (dB) versus the height and the distance; on the right, propagation factor F (db) versus height.

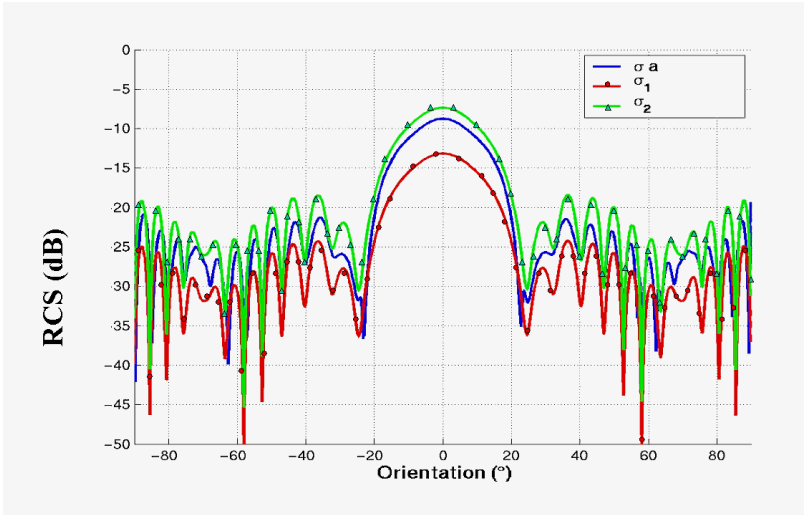

Figure 8. Bistatic RCS of the cargo at 50 MHz. Comparison of the results obtained by classical (for σ_1 and σ_2) and hybrid (σ_a) methods for the first configuration (Fig. 5).

can be distinguished at low heights from 0 to 50 meters. The curve on the right is a vertical representation of the propagation factor F in dB, propagated from the transmitter to the target at a distance of 10 kilometers. At this distance, the antenna pattern factor fa is assumed to be equal to one. Two extreme points, corresponding to the top (at 30 m) and the bottom (at 0 m) of the target, are selected to compute the apparent RCS σ_1 and σ_2 through the classical approach, according to:

$$\begin{cases} \sigma_1 = \sigma_{fs} F_1^4 \\ \sigma_2 = \sigma_{fs} F_2^4 \end{cases} \tag{21}$$

On the other hand, the real apparent RCS σ_a is calculated after our coherent hybrid method. Fig. 8 shows the final comparison results for the first case (see Fig. 5) where the target is symmetrically seen from the transmitter. The symmetry is also observed on the RCS variations around the orientation 0°. The RCS values σ_1 and σ_2 are extreme values of the classical approach and the real apparent RCS σ_a obtained is, as expected, between σ_1 and σ_2. It is only if a mean value had been chosen for the propagation factor that the classical approach would have given about the same results than the hybrid method, and then we could conclude in this case that the classical approach could give acceptable results.

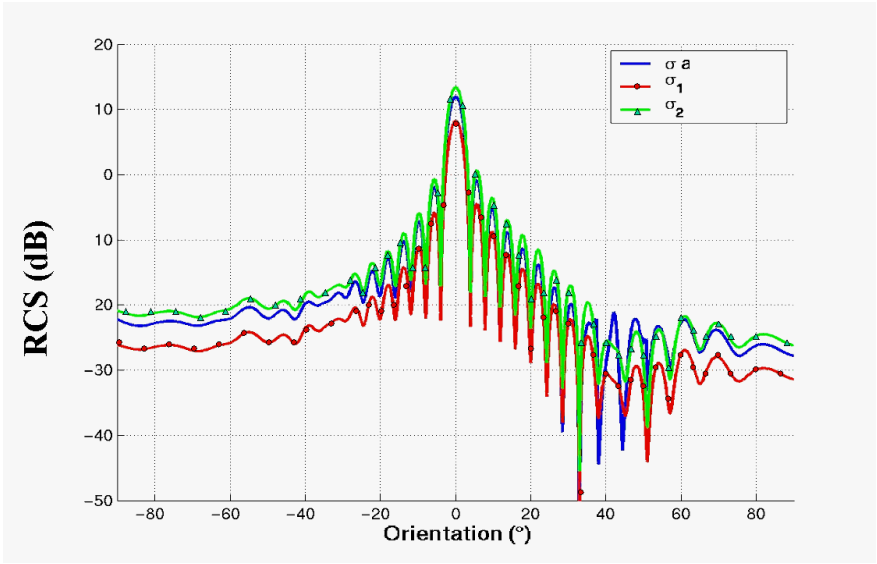

Figure 9. Bistatic RCS of the cargo without cabin at 50 MHz for the second configuration (Fig. 6).

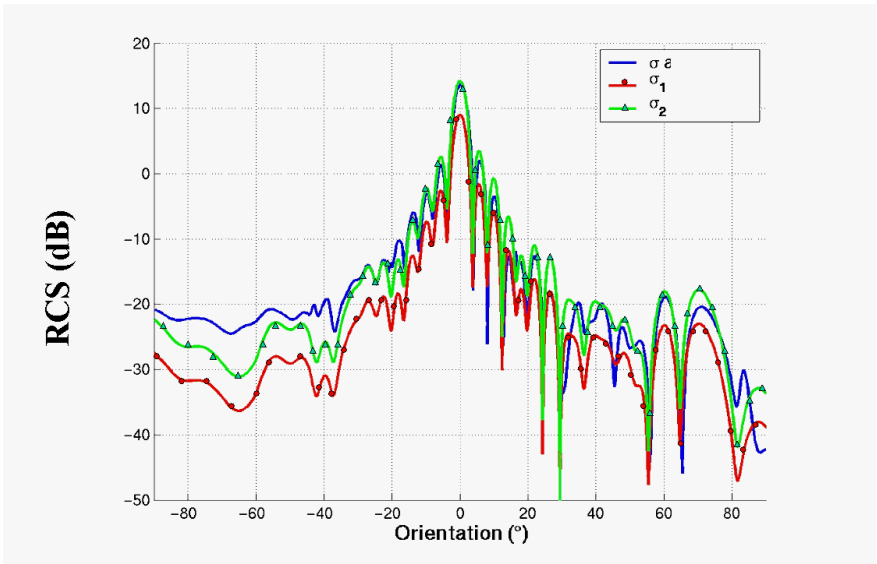

Figure 10. Bistatic RCS of the complete cargo at 50 MHz for the second configuration (Fig. 6).

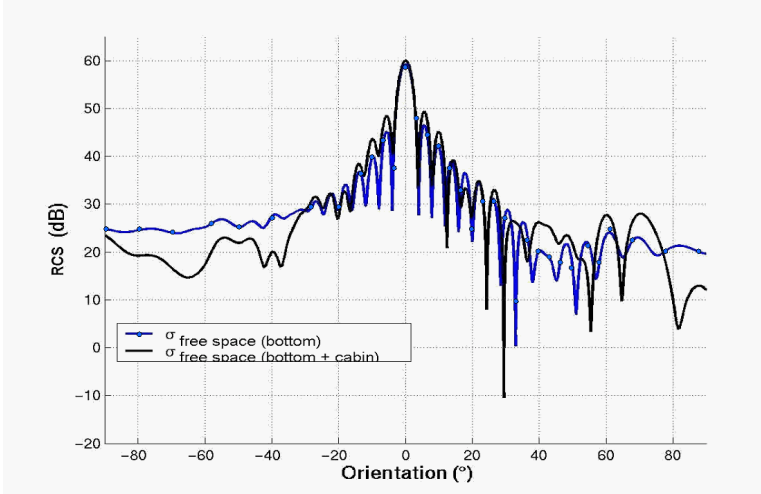

Figure 11. Cabin influence on the RCS behaviour for the second configuration (Fig. 6) on the hypothesis of free space propagation.

The second case considered corresponds to Fig. 6 where the cargo is illuminated on its side. First, if one applies the hybrid and the classical methods when the point target is only the bottom of the cargo, the apparent RCS σ_a obtained is between the extreme RCS σ_1 and σ_2 as shown on the Fig. 9. But in the same configuration and considering the complete cargo (composed of the bottom and the cabin) the results (Fig. 10) are completely different in certain angular domain. This is due to the combinations of the scattered fields generated by the bottom and the cabin. For orientation observations from $-90°$ to $-35°$, the apparent RCS σ_a obtained by the hybrid approach is above the maximum value computed by the classical approach σ_2. The reason is the following one: the bottom of the cargo is more strongly illuminated by the surface wave than the cabin and the recombination of the two scattered fields in opposite phases is less destructive because the cabin contribution is lower than the bottom one. This phenomenon is intrinsically taken into account in the hybrid approach and explains the different results obtained. This simple example shows that *the classical method can not give the right result because the target is assumed uniformly illuminated*. The maximum error involved by the classical method is 10dB and could be higher if the target were composed of several parts illuminated by different levels of the illumination law of the incident wave. This reveals the interest of the hybrid method that considers the global problem and takes into account the actual

variations of the illumination law.

A last example is given below (Fig. 11) to demonstrate the importance of the relative phases of the fields due to the cabin and the bottom. Fig. 11 shows the RCS of the complete cargo and the RCS of the cargo without cabin, on the hypothesis of free space propagation. It appears that the cabin response is combined in phase with the bottom response for orientation angles around 60° and 70°, and in opposite phase for orientation angles around 40° and 80°. For the orientation angles lower than −30°, we see that the recombination of the scattered fields from the bottom and the cabin are in opposite phase.

5. CONCLUSION

A hybrid method to evaluate the apparent Radar Cross Section of a complex target in its environment is proposed. The hybridization consists in applying the Parabolic wave equation method to calculate the propagated field incident on the target and a 3D EFIE resolution method to perform the scattered field calculation. The hybridization has been compared to the classical approach which consists in decorrelating the propagation and backscattering computation, through the product of the propagation factor and the radar cross section in free space. The example chosen were presented for a realistic surface wave radar scenario, and the final results show the limit of the classical approach when the target is large and when a non-uniform incident wave illuminates specific parts of the target more than others. We have thus demonstrated the interest of a coherent approach like the hybrid method to compute the apparent RCS of a complex target and to take into account the amplitude and phase variations of a non uniform incident wave.

ACKNOWLEDGMENT

The authors would like to thanks Dr. Gobin Vincent and Mr. Volpert Thibault for providing the EFIE resolution tool ELSEM3D and for their help.

REFERENCES

1. "Special section on over-the-horizon radar technology," *Radio Science*, Vol. 33, 1043–1266, July 1998.
2. King, W. P., "Surface-wave radar and its application," *IEEE Transactions on Antennas and Propagation*, Vol. 51, No. 10, Oct. 2003.

3. Sevgi, L., A. Ponsford, and C. H. Chan, "An integrated marine surveillance system based on high-frequency surface wave radars, Part 1: Theoretical background and numerical simulations," *IEEE Antennas and Propagation Magazine*, Vol. 43, No. 4, Aug. 2001.
4. Sevgi, L., "Stochastic modelling of target detection and tracking in surface HF radar," *Int. Journal Num. Model.*, No. 11, 167–181, 1998.
5. Khan, R., et al., "Target detection and tracking with a high frequency ground wave radar," *IEEE J. Oceanic Eng.*, Vol. 19, No. 4, 1994.
6. Patterson, W. L., *Advanced Refractive Effects Prediction System (AREPS)*, Version 1.0 Users Manual, Technical Document 3028, Space and Naval Warfare Systems Center, San Diego, CA 92152-5001, 1998.
7. Levy, M. F. and K. H. Craig, "TERPEM propagation package for operational forecasting with EEMS," *Proceedings of the 1996 Battlespace Atmospherics Conference*, Technical Document 2938, NCCOSCC, RDT&E Division, San Diego, 1996.
8. Fabbro, V., N. Guillet, and P. F. Combes, "Innovative improvements of the Parabolic Wave Equation method for radiowave propagation modeling," *ICAP 2003, Exeter*, Avril 2003.
9. Simon, J., "Extension des méthodes multipoles rapides: résolution pour des seconds membres multiples et applications aux objets diélectriques," Ph.D. thesis, Thèse Université de Versailles St Quentin en Yvelines, June 2003.
10. Chew, W. C., J. M. Jin, and C. C. Lu, "Fast solutions methods in electromagnetics," *IEEE Transactions on Antennas and Propagation*, Vol. 45, 1997.
11. Burkholder, R. J., M. R. Pino, and F. Obelleiro, "A Monte Carlo study of the rough sea surface influence on the radar scattering from two dimensional ships," *IEEE Antennas and Propagation Magazine*, Vol. 43, No. 2, 2001.
12. Bolomey, J. C., "Réponse d'une antenne de réception une onde incidente non plane," *Annales des Télécom.*, Vol. 34, No. 9–10, 469–476, 1979.
13. Fabbro, V., N. Douchin, and P. F. Combes, "Three-dimensional backscatering by a target above the sea surface," *Electromagnetics*, Vol. 21, No. 6, 451–466, 2001.
14. Dockery, G. D. and J. R. Kuttler, "An improved-boundary algorithm for Fourier split-step solutions of the parabolic wave equation," *IEEE Trans. Antennas and Propag.*, Vol. 44, No. 12,

1592–1599, 1996.

15. Kuttler, J. R. and R. Janaswamy, "Improved Fourier transform methods for solving the parabolic wave equation," *Radio Science*, Vol. 37, No. 2, 2002.
16. Donohue, J. and J. R. Kuttler, "Propagation modeling over terrain using the parabolic wave equation," *IEEE Trans. Antennas and Propag.*, Vol. 48, 260–277, Feb. 2000,
17. Leontovitch, A., "On the approximate boundary conditions for an electromagnetic filed on the surface of well-conducting bodies, investigations of propagation of radio waves," Academy of Science, Moscow, U.S.S.R, 1948.
18. Barrick, D. E., "Theory of HF and VHF propagation across the rough sea, 1. The effective surface impedance for a slightly rough highly conducting medium at grazing incidence," *Radio Science*, Vol. 6, 517–526, 1971.
19. Barrick, D. E., "Theory of HF and VHF propagation across the rough sea, 2. Application to HF and VHF propagation above the sea," *Radio Science*, Vol. 6, 527–533, 1971.
20. Phillips, O. M., "Spectral and statistical properties of the equilibrium range in wind generated gravity waves," *J. Flui. Mech.*, Vol. 156, 505–531, 1985,
21. Millington, G. and G. A. Isted, "Ground-wave propagation over an inhomogeneous smooth earth: Part 2. Experimental evidence and practical implementation," *Proc. IEE*, Vol. 97, Pt. III, 209–221, 1950.
22. Wu, Z., et al., "Recovery effect in radiowave propogation," *Electronic Letters*, Vol 26, No. 3, 162–163, Feb. 1990.
23. Norton, K. A., "The propagation of radio waves over the surface of the earth and in upper atmosphere," *Proc. IRE*, Vol. 25, 1203–1236, 1937.
24. Maclean, T. S. M. and Z. Wu, "Radiowave propagation over ground," *Chapman and Hale*, 1993.
25. Fabbro, V., "Diffraction d'une onde électromagnétique par une cible plongée dans un milieu hétérogène. Application la détection radar basse altitude au-dessus de la mer," Ph.D. thesis, Université Paul Sabatier, Toulouse, October 1999.
26. Soudais, P., H. Steve, and F. Dubois, "Scattering from several test-objects computed by 3D hybrid IE/PDE methods," *IEEE Trans. Antennas and Propag.*, Vol. 47, No. 4, 646–653, Avril 1999.
27. Knott, E. F., J. F. Shaeffer, and M. T. Tuley, *Radar Cross Section*, Artech House, 1985.

28. Moore, J. and R. Pizer, *Moment Methods in Electromagnetics*, Research Studies Press LTD, John Wiley and Sons Inc., 1984.

Vincent Fabbro was born in Le Havre, France in 1972. He received the *Diplôme d'Etudes Appronfondies (D.E.A)* degrees from the *Ecole Nationale Supérieure de l'Aéronautique et de l'espace (SUPAERO),* in 1995, and the Ph.D. degrees in electronics from the Paul Sabatier University of Toulouse in 1999. He has been working since november 1999 for the *Office National d'Etude et de Recherches Aérospatiales (ONERA)* at the Electromagnetism and Radar Department where his research activities focus on modeling radiowave propagation effects for radar and telecommunication systems applications.

Paul F. Combes was born in France in 1943. He received the *'Doctorat de* $3^{ième}$ *cycle'* from the Toulouse University, France, in 1968, and *'Doctorat d'Etat es Sciences'* from the same university, in 1978. Since 1980, he had been a Professor of microwave engineering and Head of the Microwave Antennas and devices Laboratory, Toulouse University. He is also in charge of the doctoral training in "microwave and optical telecommunication." He has been the thesis director of 30 theses and is actually conducting three theses. He is author or coauthor of about 100 publications covering the fields of reflector and arrays antennas, propagation of electromagnetic waves, radar, and radiometric and polarimetric devices for millimeter waves. In addition, he is the author of 8 books, including: *'Microwaves Transmission for the Telecommunication'* (New York: Wiley, 1991 2nd ed., 1995), *'Microwaves Componen, Devices and Active Circuits'* (New York: Wiley, 1987) and *'Micro-ondes: Lignes, Guides et Cavités-Volume 1'* and *'Micro-ondes: Circuits Passifs, Propagation, Antennes-Volume 2'* (Paris, France: Dunod, 1996, 1997, in French).

Nicolas Guillet was born in Meudon La Foret, France on December 27, 1975. He received both from the University Paul Sabatier (Toulouse, France): the *Diplôme d'études Appronfondies (D.E.A.)* degree in 2000 and the *Ph.D. Degree in Microwave Electronics*, in 2003. During his thesis he worked at the Electromagnetic and Radar Departement of the Office National d'Etudes et de Recherches Aérospatiales (ONERA) on the diffraction of an electromagnetic wave on a target in naval environment.